AIAA 96-0388

Electro-Thermal Ice Protection of a Surveillance Aircraft Radome

John K. Smith
Cox & Company, Inc.
New York, NY

34th Aerospace Sciences
Meeting & Exhibit
January 15-18, 1996 / Reno, NV

Electro-Thermal Ice Protection of a Surveillance Aircraft Radome

John Smith
Project Engineer
Cox & Company, Inc.
New York, New York

Abstract

This paper details the design and radar range testing of an electro-thermally ice protected radome. The system consists of a Westinghouse APG-66SR flat plate, horizontally polarized antenna installed inside a thin wall, nose mounted radome on a Pilatus Britten-Norman BN2T-4R Defender Aircraft. The radome is a 62" by 50" by 0.040" spheroid with an embedded 18" by 28" wire heater element centered within the impingement zone. Heater design was based on polarized radar theory that says if the heater elements are sufficiently small in diameter, spaced wide enough apart, and horizontally aligned, the heater will be transparent to the radar. Icing design was based on test data, NACA Technical Note 3587 *Impingement of Water Droplets on a Sphere* and classical thermal analytical methods. The problems solved in the design of this system include minimizing vertical wire components, maintaining constant thickness in the heated and unheated areas, and radar transparent power busing for a 2800 Watt, 28 VDC heater.

Aircraft and Radar System Description

Westinghouse and Pilatus Britten-Norman teamed to develop a low cost surveillance aircraft using the BN2T Defender equipped with Allison 250 turboprop engines and a customized radome mounted on the nose of the aircraft as shown in Figure 1. The Defender is a high wing twin engine utility aircraft weighing less than 12,500 pounds. Westinghouse installed an AN/APG-66R multimode radar, a WF-360 Forward Looking Infrared Sensor (FLIR) and Low Light Level Television Camera (LLLTV) to create the Multi-Sensor Surveillance Aircraft (MSSA). The system of interest - the AN/APG-66R radar - is a derivative of the F16 radar. The antenna is a 52" by 36" horizontally polarized flat plate array, 2.5 times larger than the F16s. It is mounted inside a 62" by 50" spheroid shaped radome.

There are three basic types of radome designs - thin wall, half wavelength and double wall. This particular radome uses the thin wall design, since the low air speed imparts only small aerodynamic loads. It is also the lightest weight and most cost effective design. The required thickness for a thin wall design is determined from Figure 2 and the radar's frequency. The AN/APG-66R operates at 9.8 GHz. Therefore, the wavelength is given by

$$\lambda \text{ (in)} = 11.8/f \text{ (GHz)} = 1.20 \text{ inches}$$

To satisfy the relationship for thin walled radomes from Figure 2 for 90% power transmission with dielectric constant (ε) between 2 and 4, the radome thickness (d) must be between

$$d = .03\ \lambda = 0.036 \text{ inches}$$
$$d = .05\ \lambda = 0.060 \text{ inches}$$

The materials used to construct the radome consisted of Kevlar fabric and a modified epoxy resin. The dielectric constant for this laminate is approximately 3.5. Therefore, the radome must be a constant thickness of approximately 0.040 inches thick (1 millimeter).

After designing the radome, the question of how to obtain certification for flight into known icing under FAR requirements or to provide some protection for military or government use arose. This aircraft's role and flight capabilities place it directly in the worst altitude range for icing conditions. However, the unmodified airframe is fully certificated and only the modified radome needs to be considered. Ice accreted on the radome could be shed into the propellers and will prevent the radar from functioning correctly.

Typically, radomes are ice protected using fluted hot air passages between two thin walls, but the additional cost, weight, and unavailability of bleed air discounted the traditional approach. There were three alternatives available - a pneumatic boot, a fluid freezing point depression system sprayed from a boom protruding several feet in front of the radome (a unicorn horn) or an electric heater embedded directly in the radome. The pneumatic boot was discounted because its thickness would attenuate the radar signal and the debris released would pass through the propellers.

Since the radar is polarized, it is possible to run evenly spaced, parallel conductor strips in front of the antenna without affecting its performance. Analysis performed by Westinghouse showed that if conductor spacing remained less than 12 per inch and conductor width less than 0.007 inches, the power transmission would be decreased by less than 3 percent.

Since the electro-thermal approach was theoretically possible and its impact on aircraft weight, structure and appearance were minimal, this protection method was selected and explored.

Impingement Analysis

Impingement limits and collection efficiencies were determined analytically using the methods described in NACA 3587 *Impingement of Water Droplets on a Sphere* [Ref. 1]. The impingement limits were computed using 40μ droplets and collection efficiencies calculated using 20μ droplets. Free stream Reynolds number with respect to the droplet (Re_o) and the inertia parameter (K) were calculated for each case. The resulting impingement limits are shown in Table 1 and were derived from Figure 3. Collection efficiency, which starts at about 0.1 and decreases down to 0 within 7.5 inches of wrap, is shown in Figure 4.

Table 1
Impingement Limits Predicted from methods of NACA 3587

TAS (Knots)	MDD (μ)	Radius (in)	Re_o	1/K	Impingement Limit (wrap inches from highlight)
85	20	62	79	12.7	< 6.0
147	20	62	134	7.5	< 6.0
147	20	50	134	6.0	< 6.0
147	40	50	267	1.5	17
147	40	62	267	1.9	15

Outdoor testing was also conducted at the Bascombe Down Aeroplane and Armament Experimental Establishment (A&AEE) Facility. This facility is located in England and has an outdoor icing range which uses Merlin engines to power the blowers and liquid nitrogen for cooling. The test used a complete, full scale aircraft with radome mounted on adjustable stands to vary AOA. Results are summarized in Table 2.

Table 2
Average Wrap Distance to Impingement Limits from
Highlight from Bascombe Down Tunnel Test [Ref 2]

TAS Knots	Avg. MDD μ	AoA deg	Temp °C	Time sec	Horiz-ontal in	Vertical (in)	
						up	down
83	22	+7	-11	2705	11.5	11.5	19.6
151	22	-1.4	-11	1980	11.2	13.1	18.0
83	41	+7	-8	900	15.3	14.7	14.9
151	38	-1.4	-9	600	13.8	13.0	15.9

The NACA 3587 method predicts impingement limits of 30" by 34" for 40μ droplets and 12" by 12" for 20μ droplets. Data from the Bascombe Down tests shows impingement limits of approximately 23" by 33" for 22μ droplets and 30" by 31" for 40μ droplets. The calculated results for 40μ droplets correlated reasonably well to the test data. Discrepancies between the 20μ results are probably due to the long exposure time without deicing and the distribution of larger droplets in the test cloud. Exposure for the 22μ case was 45 minutes at 0.5 g/m^3 LWC.

Power Requirements

With the radar system functioning, the available power for radome ice protection was 100 amps at 28 volts DC (2800 Watts). Using the classical solutions for film coefficient on a sphere and an iterative solution for total evaporation, the power requirements for total evaporation at 147 knots (aircraft maximum airspeed) were determined as shown in Table 3.

Two power zones were chosen, an inner zone (~12" by ~12", 125 in^2) using 8.5 watts/in^2 and an outer zone (the outside of ~18" by ~28", 300 in^2) using 4.5 watts/in^2. This 2500 watt heater should provide complete evaporative protection for FAR 25 Continuous Maximum (CM) Icing and running wet protection for Intermittent Maximum (IM) Icing. The effect of repeated exposure to IM conditions would be a run back ridge outside the heater. This condition could be defeated with a hold time limitation either in icing conditions or by adding a deicing band around the outside of the heater. If a deicing band is found necessary, it could be powered by temporarily shutting off the radar systems.

Table 3
Calculated Power Requirements

OAT F	h BTU/ hr.ft^2.F	LWC g/m^3	Beta	Power for total Evaporation W/in^2
-22	25.2	0.14	.075	4.53
-4	25.2	0.21	.075	4.85
14	25.2	0.42	.075	6.97
32	25.2	0.63	.075	8.73
32	19.4	0.63	.033	4.16

System Temperature Control

Radome surface and internal temperature analysis were conducted using Algor FEA software to determine the effects of operating the system dry, thermal gradients on the surface and the type of temperature control system that would be required. Results of the analysis show the maximum surface temperature at 85 knots airspeed and 40°F ambient to be approximately 300°F (Figure 5).

Since all the materials used in the radome can handle this operating temperature continuously, the system can run open loop with a simple mechanical relay for power engage/disengage. A heater thermostat, Outside Ambient Temperature (OAT) thermostat, and Weight on Wheels (WOW) signals are connected in series with the relay coil to provide over temperature protection. The heater thermostat location would be approximately 10" above the highlight of the

radome. This location would not interfere with the radar, since it is out of the operating line of sight. The system would, in general, switch the 100 amps only at activation and shutoff - once or twice per flight.

Heater Design

The primary problem in the heater design was to get the power to the heater elements without affecting the radomes transmission characteristics while creating the different power density zones. Because the radar is significantly affected by vertical bus bar arrangements, power had to be supplied in horizontal leads brought around from the sides of the radome. For reference and a possible cost savings, a curved vertical bus arrangement was also simulated.

The bus arrangement difficulties were further compounded by the available 28 VDC power supply. Because power is equal to the voltage squared divided by the circuit resistance, low voltage heaters require low resistivity conductors (with correspondingly large diameters). Since the radar could not tolerate element diameters larger than 7 mils at the element spacing required, numerous parallel heater circuits had to be used.

An additional design challenge was to minimize the number of vertical end loops in the heater circuits. This was accomplished by using long runs of Cox's Thermowire™ as the heater element. Thermowire™ is a braided, strain relieved conductor assembly. It allows the conductor to "float" in a jacket assembly which takes the majority of the stresses created by thermal cycling as well as structural loading.

After considering all these factors, a heater consisting of 81 parallel circuits was designed. Two samples were manufactured - a lead less, nonfunctional unit and a fully functional assembly which used 42 horizontal leads run from the heater edge back to the vertical fuselage attachment point of the radome. A simplified illustration of the heater designs considered is shown in Figure 6. Three forward half radome samples were fabricated and tested in four configurations:

Sample 1 - Plain Kevlar\Epoxy
Sample 2 - Non-functioning, lead less heater
Sample 3 - Horizontal lead heater
Sample 4 - Sample 2 with curved power bus

The lay up around the 18" by 28" heater was modified to maintain thickness consistent with the rest of the radome and near equivalent structural properties.

Radar Range Test & Results

The sample was mounted in front of the APR-66 antenna and tested at the Westinghouse Hardy outdoor radar range. The test sequence consisted of elevation and azimuth sweeps at different antenna gimble angles. Relative power plots were generated for the bare antenna, the unheated control radome half and the heated radome halves. Figure 7 shows the samples installed at the range.

Significant items which affect the radar performance are the loss in gain, the level of side lobes and the overall noise level. Loss in signal strength and increased noise decrease the range and resolution of the radar. Side lobes cause false images or false locations for actual targets. The typical thin wall radome effect on the radar signal is shown in Figure 8.

Both the heated and unheated radomes produced a signal strength loss of approximately 0.3 dB relative to the bare antenna. Only the curved vertical bus arrangement (sample 4) produced significant signal loss, approximately 1 dB.

The sweep patterns of the samples (except sample 4) closely matched the patterns of the bare antenna. All the side lobe levels were below -35 dB in azimuth sweeps and -30 dB

in elevation sweeps. The overall noise levels (the area under the sweep pattern) are slightly higher than those of the bare array, resulting from somewhat higher outer lobe levels. However, the outer lobe levels were still below -45 dB.

The curved vertical bus arrangement of sample 4 produced significant increases in side lobe levels. The first side lobes increased 3 to 5 dB over the other samples. The general noise levels were also significantly increased. Based on this, all forms of vertical bussing for power were discounted.

Figures 9 to 12 illustrate the typical relative power vs. off axis angle from this test.

Most of the performance differences between the bare antenna and the patterns produced by the specimens can be attributed to the addition of the thin wall of the radome itself. The addition of the heater elements and horizontal leads had little effect when compared to the unheated radome.

Thermal Verification

Ice accretion shapes were determined at the Bascombe Downs test. Verification of the thermal performance - tunnel and flight tests - remains to be completed.

Conclusion

From a radar signal standpoint, the patterns produced by a thin wall radome with an integrally molded, horizontal lead heater circuit are acceptable. From an ice protection standpoint, the system will theoretically work on the estimated 2800 watt power budget.

Depending on the specific type of radar system, an electrothermal system can be a viable means of providing ice protection to the radome.

References

1. R. G. Dorsch, P. G. Saper, and C. F. Kadow, *Impingement of Water Droplets on a Sphere* NACA Technical Note 3587, 1955.

2. R. J. Gould, *PBN Islander Astor Radome Icing Trial*, Letter Report E907, 1990.

3. *Radome Engineering Handbook*, Walton(editor), Marcel Dekker.

4. *Antenna Engineering Handbook*, Jasik(editor), McGraw-Hill.

5. *Test Report: Radar Transparency of Electro-Thermally Anti-Iced Radome*, Cox & Company Document D-9210, 1994.

Figure 1
The PBN/Westinghouse Multi-Sensor Surveillance Aircraft (MSSA)

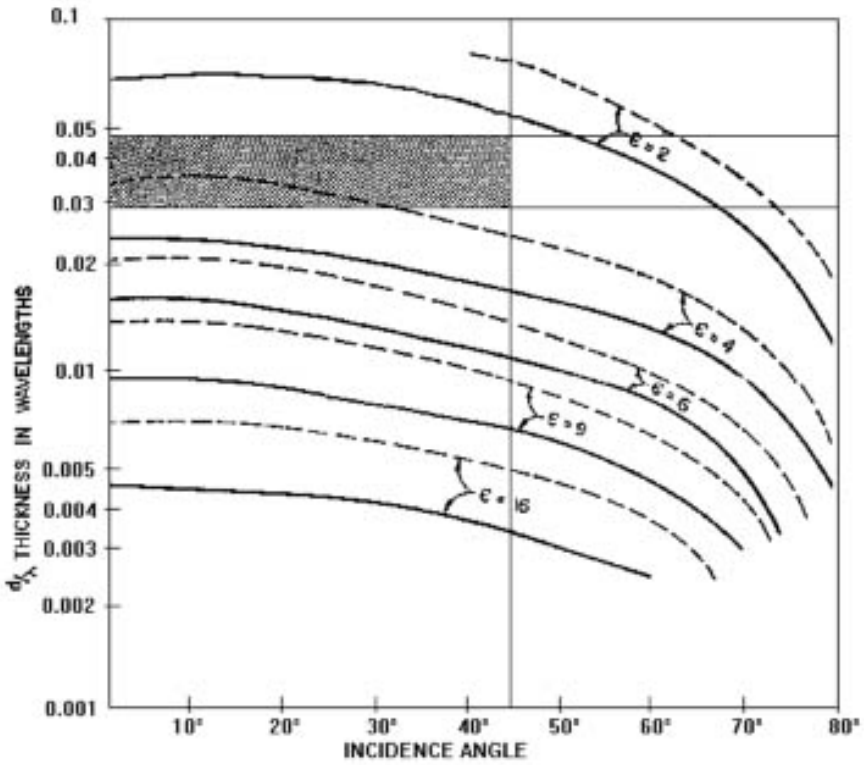

Solid = 95% Transmission Dashed = 90% Transmission
Figure 2
Thin Wall Radome Maximum Thickness/Wavelength based on Material Dielectric Constant (ε) [Ref. 3]

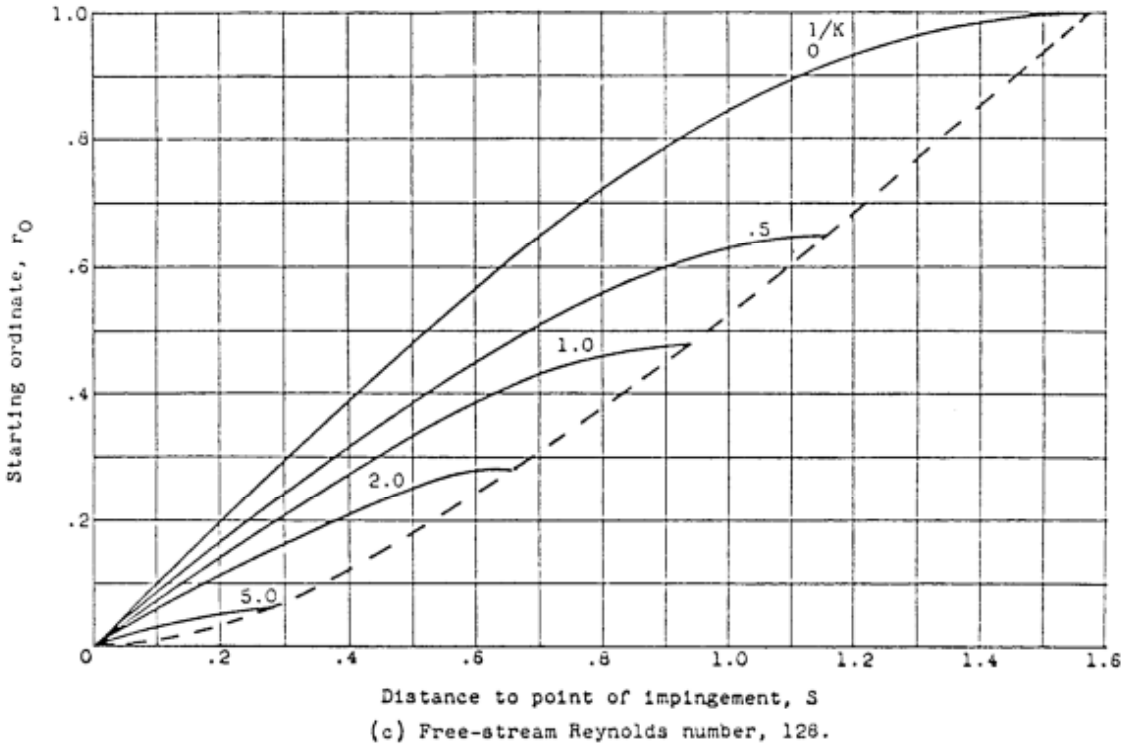

(c) Free-stream Reynolds number, 128.

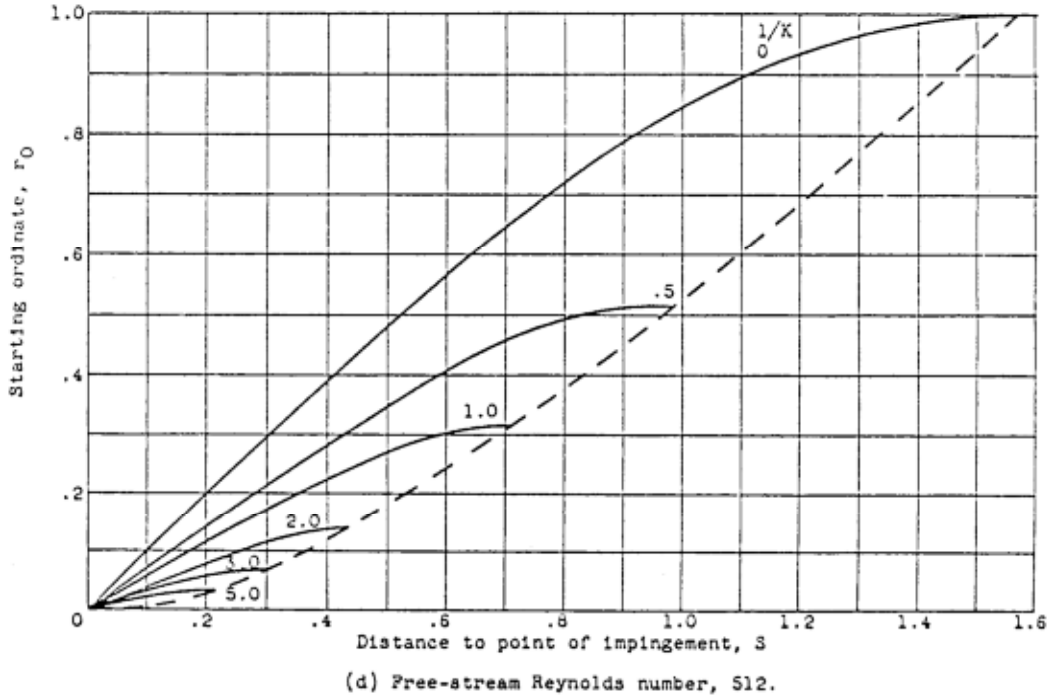

(d) Free-stream Reynolds number, 512.

Figure 3
Impingement Limits of a Sphere [Ref. 1]

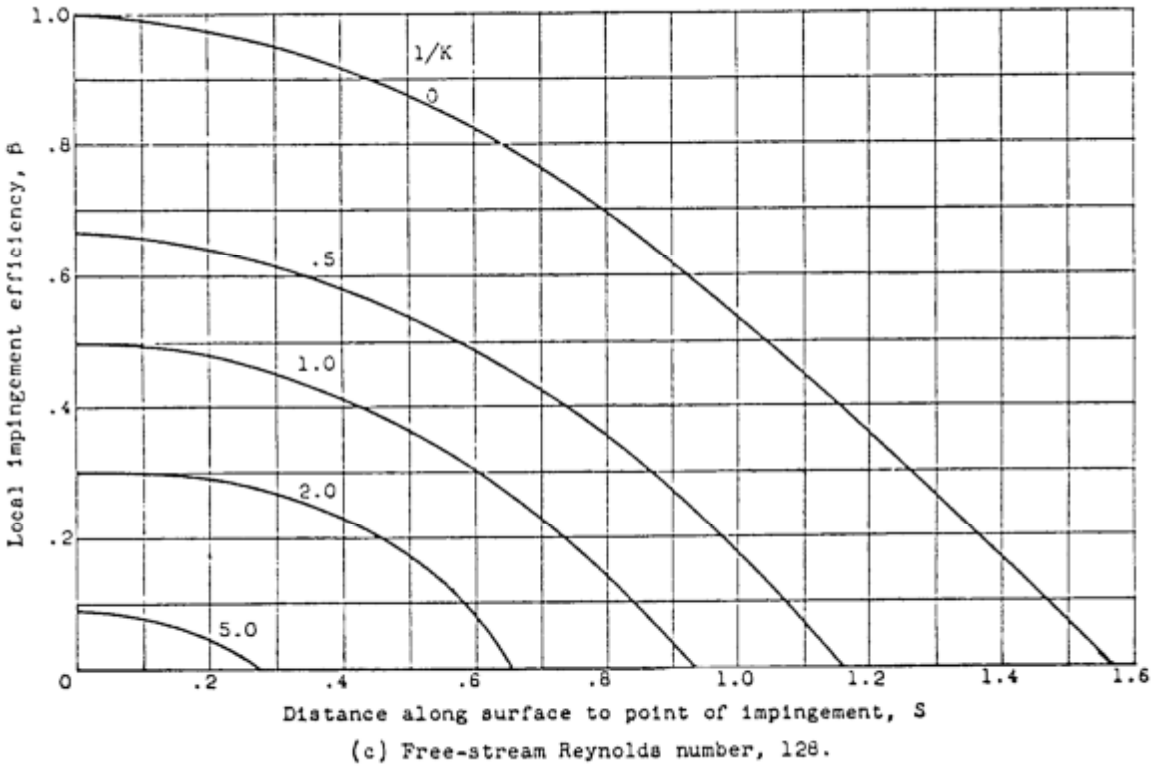

Figure 4
Local Collection Efficiency of a Sphere [Ref. 1]

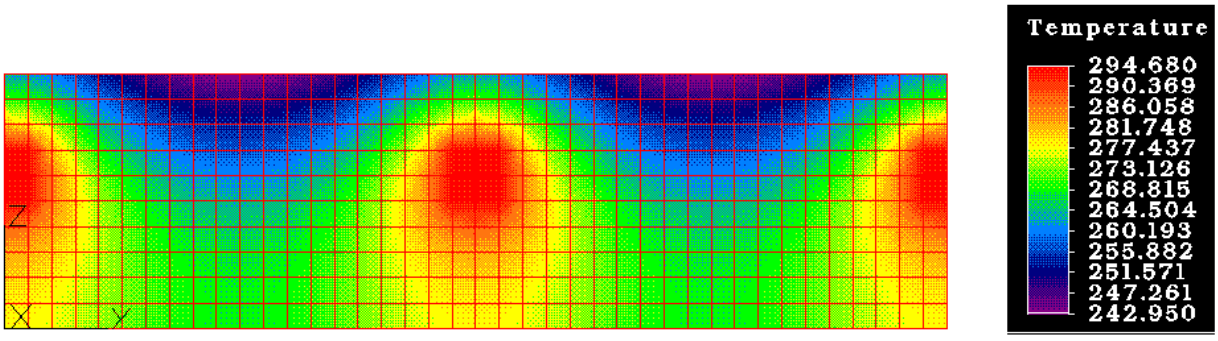

Figure 5
FEA Temperature Analysis Output
Outer Surface H=19 BTU/hr·ft^2·°F, T=243 to 262°F
Inner Surface H=1 BTU/hr·ft^2·°F, T=268 to 278°F
Power = 8.5 Watts/in^2, Tamb = 40°F

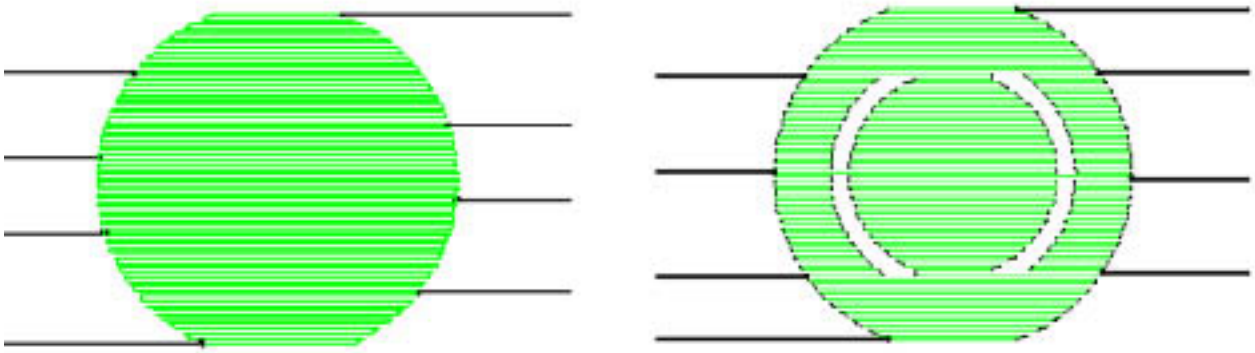

Figure 6
Example Horizontal Lead Heater Configuration

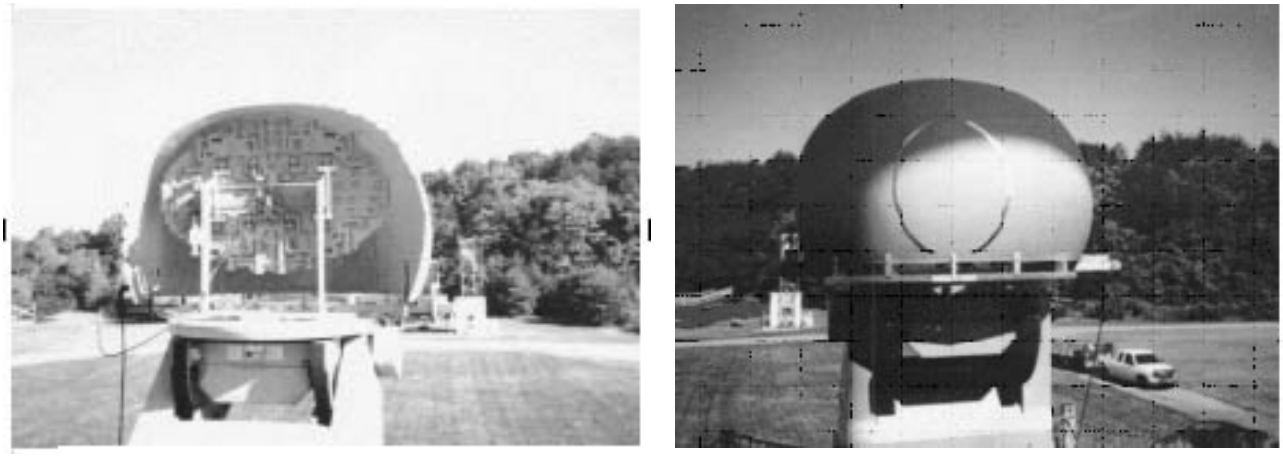

Figures 7
Sample 3 facing the range and Sample 4 after installation

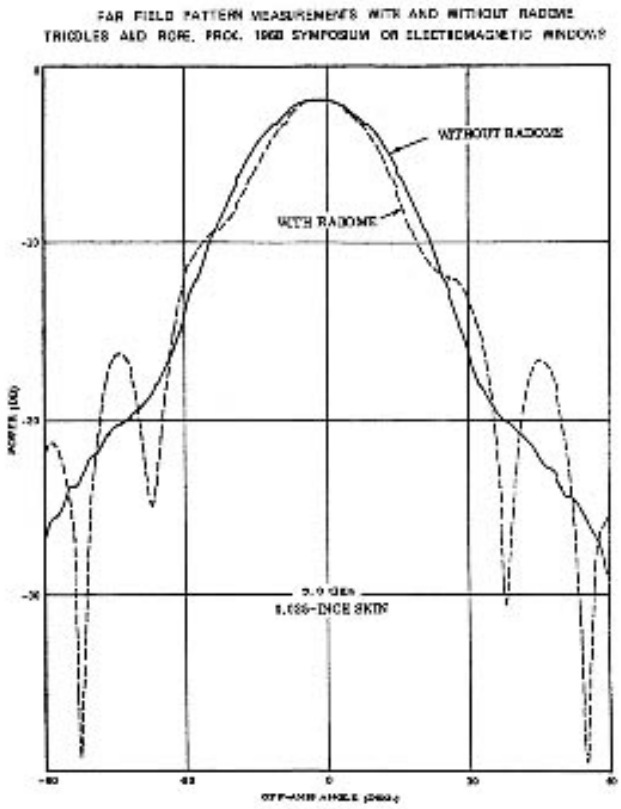

Figure 8
Typical Effects of Thin Walled Radomes on Far Field Pattern

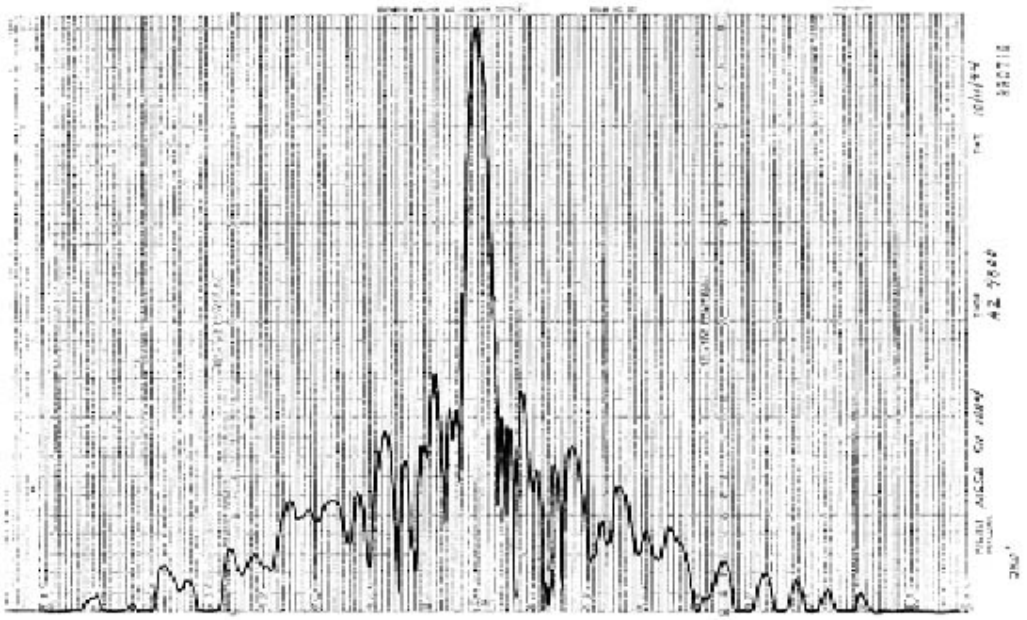

Figure 9
Bare Antenna Far Field Pattern

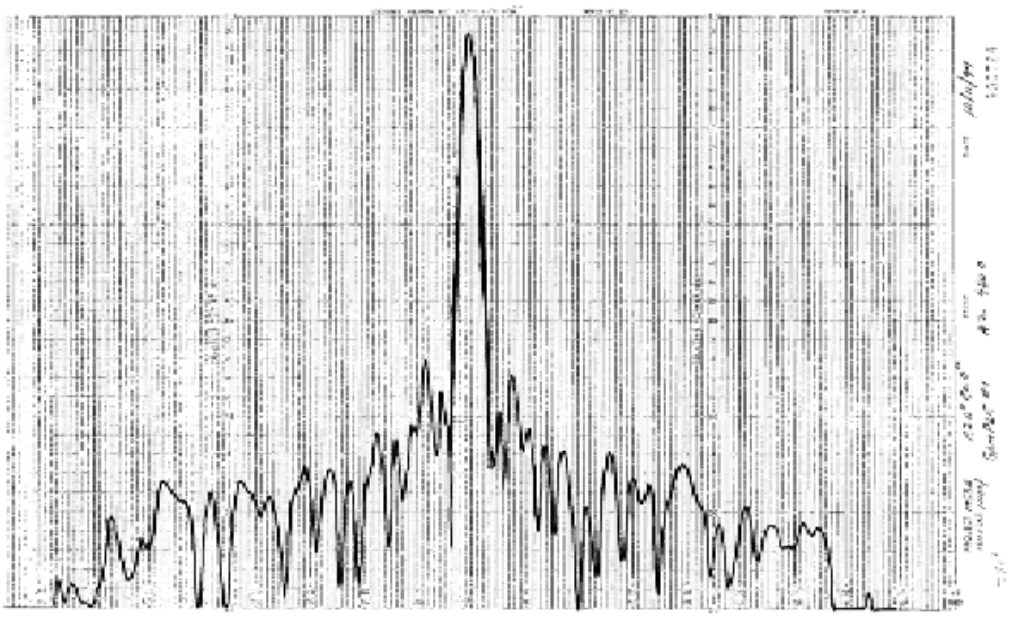

Figure 10
Sample 1 (Plain Radome over Antenna) Far Field Pattern

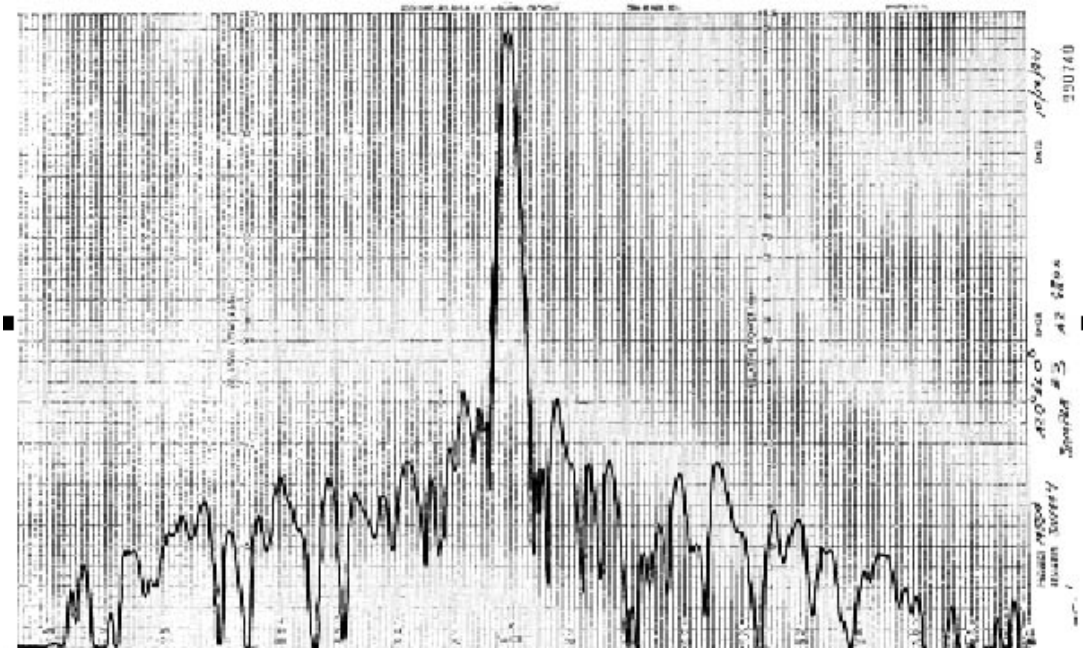

Figure 11
Sample 3 (Heated Radome over Antenna) Far Field Pattern

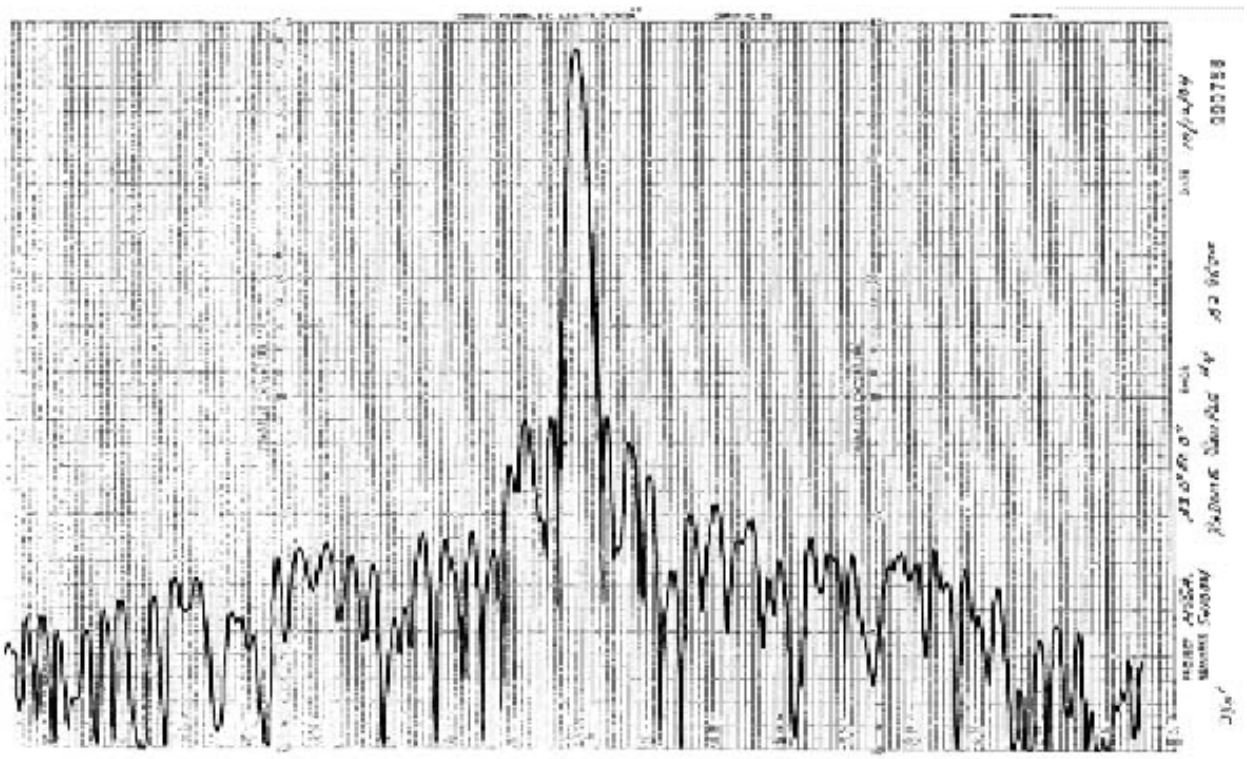

Figure 12
Sample 4 (Vertical Bus Radome over Antenna) Far Field Pattern